International Journal Of Renewable Energy Research, IJRER
M.A.Tankari, M.B.Camara, B.Dakyo, C.Nichita , Vol.1, No.2, pp.86-95 ,2011

Ultracapacitors and Batteries Integration for Power Fluctuations mitigation in Wind-PV-Diesel Hybrid System

M. A. Tankari*, M.B.Camara**, B. Dakyo***, C. Nichita****

GREAH Laboratory, University of Le Havre, Le Havre, France,
25 rue Philippe Lebon, BP 540, 76058 Le Havre Cedex France

‡ E-mail: {abdoutam*, camaram**, dakyo***, nichita****} @univ-lehavre.fr

Received:23.04.2011 Accepted:20.05.2011

Abstract- Fluctuations are induced by the wind power variations at the common coupling point of the hybrid system. The intensity of the resulting perturbations is related to the penetration ratio of the renewable energy. In this paper, wind generator and photovoltaic are combined with the diesel generator to supply energy to the DC-bus. Interactions between these sources are studied before the inserting of the ultracapacitors and lead acid batteries, for power fluctuations mitigation. To ensure a good life cost and good performance of the system, a method of storage sizing, integrating the devices lifetimes estimation is proposed. This method takes into account the system applications conditions. The experimental test bench is designed in a reduced scale, and some simulations and experimental results are presented and analyzed.

Keywords- Battery, diesel generator, photovoltaic power, storage device, ultracapacitors, wind power.

1. Introduction

Nowadays, renewable energies are considered as the mean to reduce fuel consumption and air pollution. But, the stochastic variations of the climatic conditions can induce several constraints in the electrical power generation system [1-3]. Energy fluctuations can have a significant effect on the design and performances of the individual wind turbines, as well as on the quality of the power delivered to the network and to the consumers.

In this paper, the wind-PV-diesel hybrid system coupling is studied and the interactions of these sources are analyzed. The significant part of the wind generator power fluctuations is located below 1Hz. Most of the high frequency fluctuations (above 1Hz) are effectively damped by the large inertia of the wind generator (WG). Their magnitudes are irrelevant [4-6]. It can be noticed that the photovoltaic (PV) power is smoothed in the cloudless conditions and the diesel engine is a slow dynamics system. So, storage devices are required to mitigate the disturbances induced by the wind generator current on the DC-bus. Ultracapacitors (UC) and Batteries are used in this aim. The system stability and autonomy is related to the storage devices capability to ensure their missions [4,7-9]. For this reason, it becomes necessary to perform a good sizing of the storage devices.

The Rainflow counting method is used to estimate the number of cycles and the storage devices lifetime. The synoptic of the studied hybrid system is presented in Fig.1. The energy management strategies are illustrated through some simulations and experimental results, which are presented and analyzed.

2. Wind and Photovoltaic Power Generation

2.1. Wind power generation

The wind speed includes a low frequencies component W_{BF} and a turbulent component W_{turb}, as expressed in (1). The power supplied by

the wind generator to DC- bus follows the variations of wind speed.

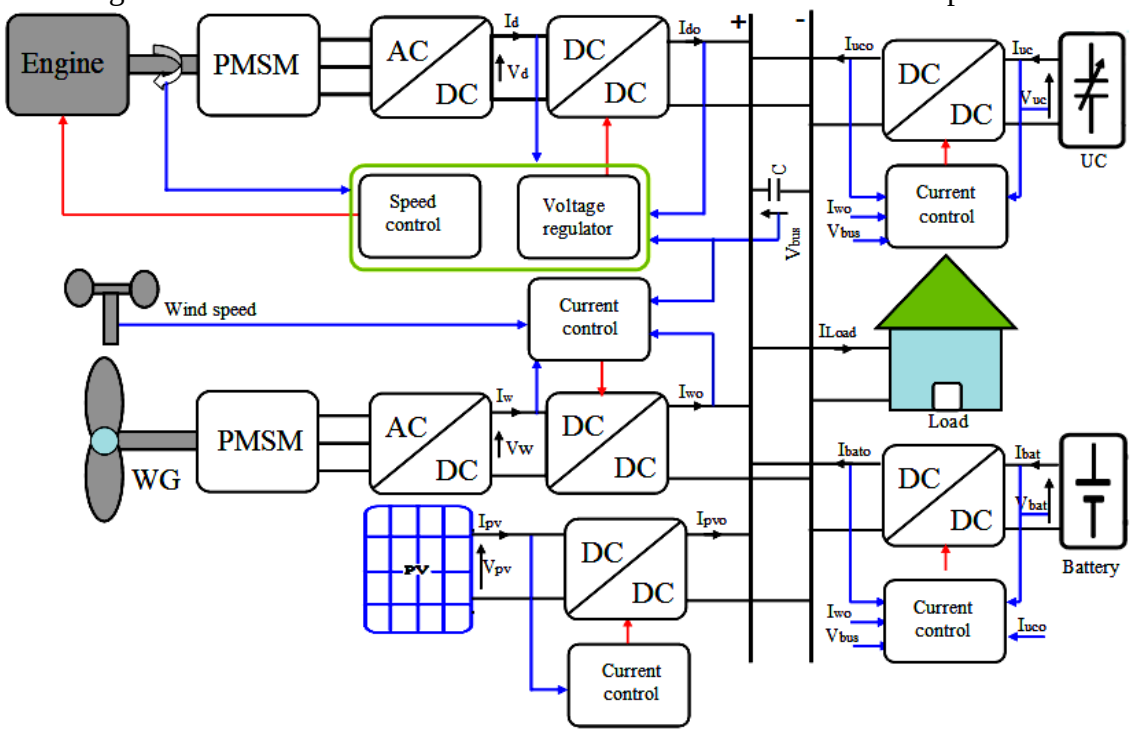

Fig. 1. Wind-PV-Diesel Hybrid system configuration.

The significant part of the wind power is located in the frequency domain below 1Hz. Most of high frequencies fluctuations (above 1 Hz) are effectively damped out by the wind generator large inertia, their magnitudes are not significant [4,6].

$$W_s = W_{BF} + W_{turb} \tag{1}$$

To generate the wind energy, a permanent magnet synchronous generator (PMSM) is driven by the wind turbine. A diodes rectifier bridge is associated with a buck converter to operate the system at its maximum power.

This solution induces a reduction of fuel consumption by the diesel generator. The used MPPT method in this study is detailed in previous works [10]. This method shows that the rectified current is a quadratic function of wind speed, according to (2).

$$\begin{cases} I_{w-opt} = K_{w-opt} \cdot W_s^2 \\ K_{w-opt} = \dfrac{1}{\sqrt{6} \cdot p \cdot \Phi_{\max}} \cdot \rho \cdot \pi \cdot R^3 \cdot C_\Gamma(\lambda) \end{cases} \tag{2}$$

2.2. *Photovoltaic power generation*

In this paper, the proposed MPPT strategy uses only the measurement of the PV current to track the maximum power. A buck converter is interfaced between the PV panel and the DC-bus to transfer the PV maximum power. The PV current is measured for each variation of the solar radiation, and the duty cycle D is estimated to switch a buck converter.

$$I_{pv} = I_{ph} - I_{sat}\left(\exp\left(\frac{V_{pv}+R_s.I_{pv}}{A.V_T}\right) - 1\right) - \frac{V_{pv}+R_s.I_{pv}}{R_{sh}} \tag{3}$$

The corresponding MPPT control law is based on the buck converter average model. The duty cycle value D can be deduced according to (4). It can be observed that for a constant DC-bus voltage, the power variation is proportional to P*.

$$\begin{cases} D = \dfrac{V_{bus}}{V_{pv}} \\ P_{pv} = V_{pv} \cdot I_{\text{pv}} = V_{bus} \cdot P* \\ P* = \dfrac{I_{pv}}{D} \end{cases} \tag{4}$$

The plot of P* as function of duty cycle shows that only one maximum power point exists for each radiation [11]. The MPPT algorithm deduced from this observation is summarized in Table I. The elementary variations ΔP* and ΔD are defined in (5). The duty cycle is incremented or decremented by a constant value Δd according to the position of the measured current I_{pv} relating to the maximum point.

$$\begin{cases} \Delta P^* = P^*(t+dt) - P^*(t) \\ \Delta D = D(t+dt) - D(t) \end{cases} \quad (5)$$

Table 1. The duty cycle is incremented or decremented according to ΔP* and ΔD signs

ΔP*	ΔD	Following step
>0	>0	+Δd
>0	<0	-Δd
<0	>0	-Δd
<0	<0	+Δd

3. Interactions on the DC-bus of a no-Storage Wind-PV-Diesel System

The disturbances induced by the wind generator on the DC bus can reduce the system performance. Analysis of these disturbances is required to ensure compatibility between the diesel generator (DG) missions with its dynamics.

In such a hybrid system, the DG system controls the DC-bus voltage. To satisfy the power required by the load, the DG is subject to the combination of the wind power and the PV power variations. This situation is analyzed through simulation results presented in Fig. 2 to Fig. 4. These simulations are carried out to analyze the interactions that occur on the DC-bus and the dynamic limits of the DG. In these simulations, the diesel engine is modelled as a first order transfer function [12,13].

In part I (Fig.2 to Fig.4), the wind speed is constant and the solar radiation varies slowly. The difference between the renewable power (wind and PV) and the load need is compensated by the DG. It can be observed a good control of the DC-bus voltage around 110V by the DG.

In part II, the wind speed contains disturbances with a frequency of 30mHz. The DC-bus voltage regulation is not sufficiently performing. It appears a periodical overshoot varying from -4.5% to +7%. The overshoot value is related to the penetration ratio of the wind power.

In part III, the wind energy contains 4Hz of disturbances. The control is very instable with an overshoot varying from -32% to +90%. The wind power variations are too faster than the DG dynamics. It can be observed that the PV power is as fluctuating as the DC-bus voltage, for a smoothed solar radiation. So, the instability of the DC-bus is propagated over the hybrid system.

In part IV, the wind energy contains 1mHz of disturbances. The DC-bus voltage is well regulated to the set point and the PV power is not polluted.

Thus, it results poor regulation of DC-bus voltage if there is incompatibility between the dynamics of DG and its mission. This can also lead to poor efficiency of the DG.

To ensure proper system performance, faster compensation of fluctuations must be ensured by using high dynamics sources, such as storage units. The storage devices are able to absorb high dynamics disturbances to improve the hybrid system performance.

4. Dedicated Sizing of Storage Devices

Sometimes, the renewable energy system is designed by only considering the storage devices lifetime estimated by the manufacturer and by using the hourly data. The impacts of actual conditions (intermittencies of wind or solar energies) in the storage devices lifetime are not taken into account. But, knowledge of renewable energy system shows that battery's lifetime is drastically reduced when operating under big number of cycles. So, it becomes important to size the storage devices by integrating the turbulent part (short-term variations) of the renewable resources in the constraints. In this context, a new method of storage units sizing is proposed in this paper. The principle of this strategy is shown in Fig.6, and explained as following:

1. Hybridization factors are applied to the specifications (wind energy potential of the location and load power) to determine whether or not storage units are necessary;

2. Various storage configurations are then studied. Three cases are possible: using only batteries or only ultracapacitors or combination of the two storage units;

3. Depending on configuration, a strategy for energy management is defined and applied to the system;

4. Simulations are then performed with Simulink software model by considering that the storage units can effectively ensure their mission;

5. The storage capacity is estimated from the simulations results. The database of manufacturers is used to select the characteristics of the storage devices. Then, the lifetime of the storage units is estimated;

6. If the determined parameters are acceptable (better than for other configurations), then the system is simulated again with more refined models of the selected storage units;

7. If the system is considered efficient (disturbances effectively absorbed by storage devices), the storage devices choice is validated, otherwise the sizing loop is computed again

4.1. Hybridization factors

The storage devices are integrated in the hybrid system in aim to optimize the system performance. Their choice must therefore meet a real need in the conditions of operation. For this, it is necessary to provide criteria for decision support that can give, to the designer, an idea about the potential reduction of fluctuations by the storage sources using.

The required characteristics (capacity, reaction time) of the storage devices dynamics depend mainly on variations of the power to be compensated by the DG. The relative variation of power, defined as the Hybridization Factor of Power HFP (6), reflects the importance of the fluctuating power compared to the average value of the DG mission. In this equation, P_{max} and P_{mean} are respectively the maximum and average powers. The system is very favourable to hybridization if PHF is equal to 1 and very unfavourable for HFP equal to 0.

$$PHF = \begin{cases} \dfrac{P_{\max} - P_{mean}}{P_{\max}} & \text{if} \quad P_{mean} \geq 0 \text{ and } P_{\max} > 0 \\ 1 & \text{else} \end{cases} \tag{6}$$

Nevertheless, it appears that two profiles of same maximum power and same average power, thus with same HFP, may contain fluctuations with different nature [14].Thus, for the same HFP, the capacity of storage units may be more or less large depending on the fluctuations speed (frequency) and their amplitudes related to the mean power. A second factor is therefore necessary in aim to take into account the nature of the disturbances contained in the mission profile of the diesel generator. The Energy Hybridization Factor (EHF) is used to express the nature (frequency and regularity) of the energy variability (8). Its value indicates the degree of difficulty to integrate the storage units in the system.

A more regular profile (the largest EHF) contains less energy to store and therefore a greater potential of hybridization. It is therefore more appropriate to the energetic hybridization of the system.

$$EHF = \begin{cases} \dfrac{P_{\max}}{\Delta E_s} & \text{if} \quad P_{\max} \geq 0 \text{ and } \Delta E_s \neq 0 \\ +\infty & \text{else} \end{cases} \tag{7}$$

The energy variation ΔE_s is estimated as presented in (8).

$$\begin{cases} E_s = \int_0^{\tau} (p(t) - p_{mean})dt \\ \Delta E_s = \max(E_s(t)) - \min(E_s(t)) \end{cases} \tag{8}$$

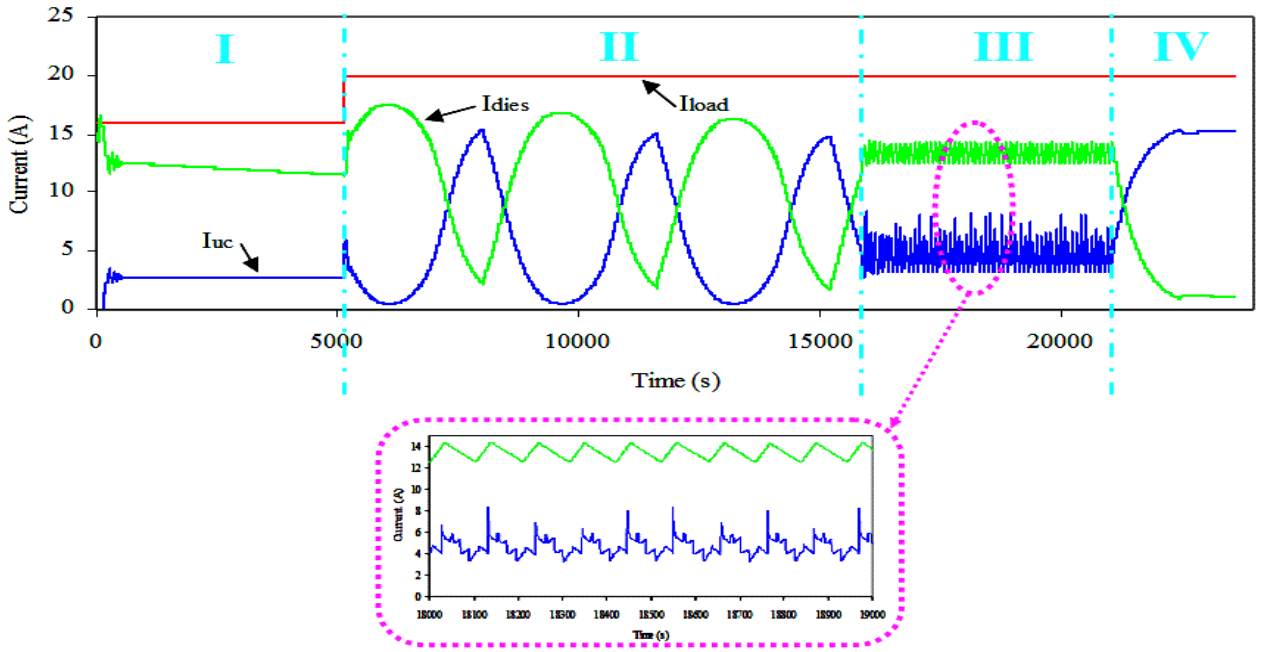

Fig. 2. Impacts of the *WG* current variations on the *DG* current for a constant load.

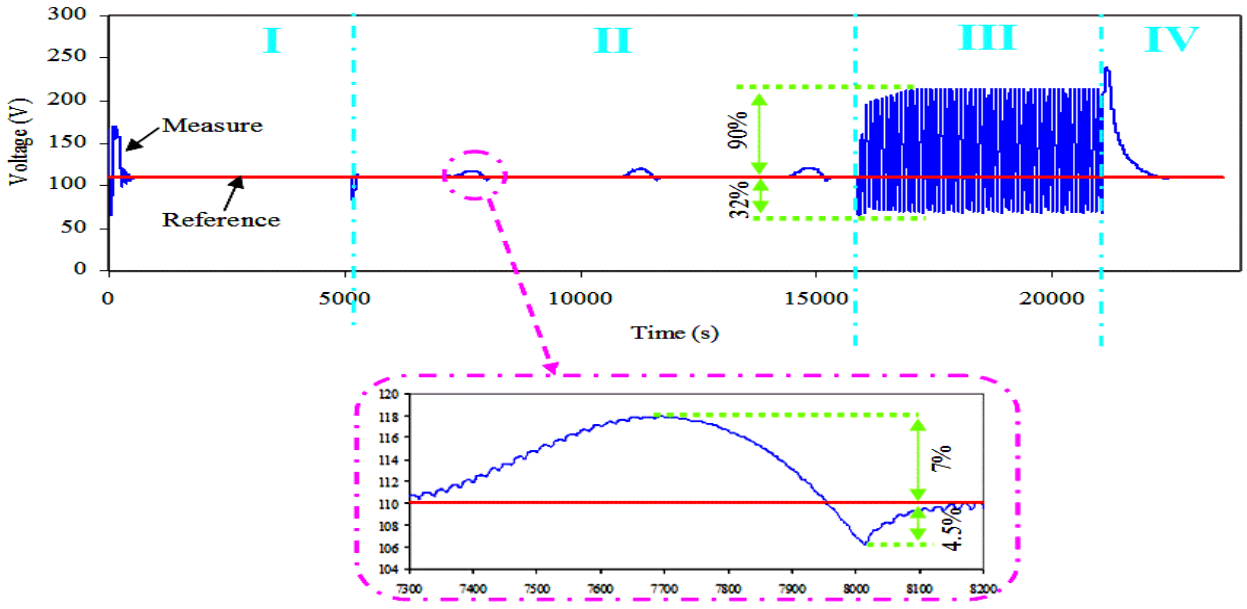

Fig. 3. Impacts of the WG current variations on the DC-bus control and the system stability.

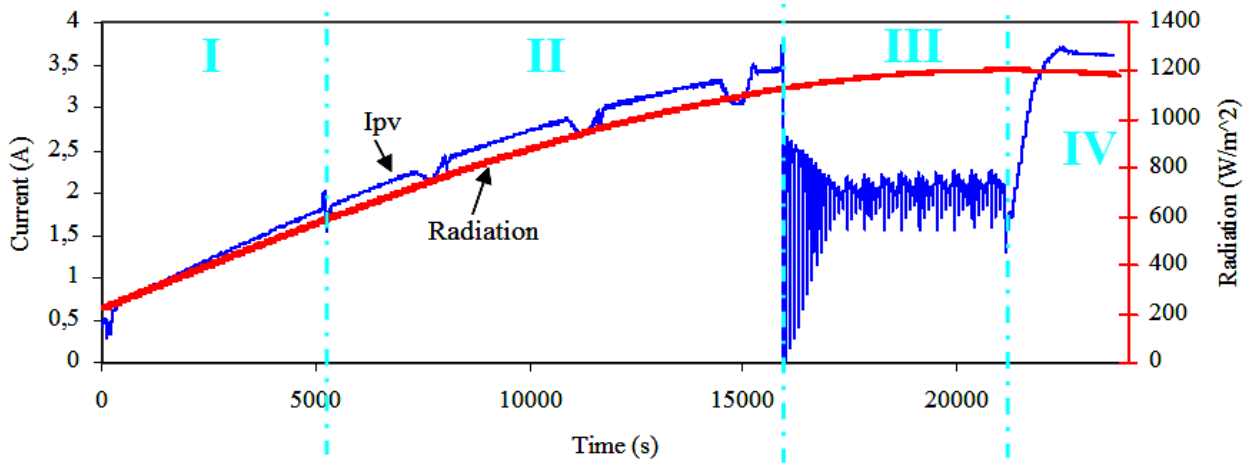

Fig. 4. Impacts of the *WG* current variations on the *PV* current for a smoothed radiation.

4.2. Ultracapacitors and battery lifetime analysis

4.2.1 Ultracapacitors lifetime analysis

The lifetime of UC is mainly affected by the combined effects of the voltage and the operating temperature [15,16]. The performance of UC decreases with the capacity decreasing or with the increasing of the resistor.

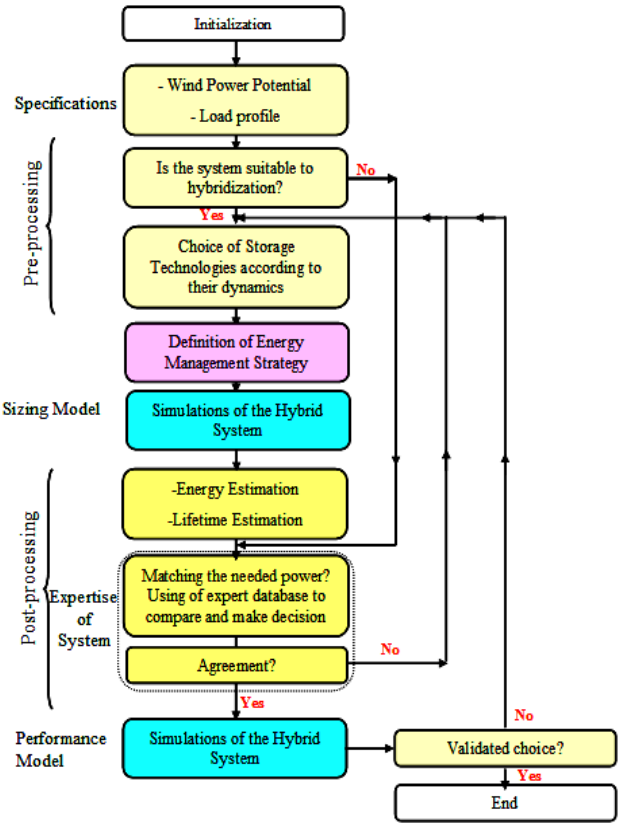

Fig. 5. Flowchart of storage devices sizing.

Thus, the end of lifetime is reached when the capacity decreases by 20% of its nominal value and / or when the internal resistor increases by 200%, according to industrial standards [15]. The lifetime of UC is less affected by the number of cycles compared to batteries ones.

4.2.2 Battery lifetime estimation

The battery lifetime is strongly affected by the number of charge and discharge cycles [17,19]. In a wind-diesel system incorporating storage units, batteries are the most affected component by the large number of micro-cycles contained in wind power. Thus, they are the weak link of the system. For this reason, it is important to take into account the effects of operation conditions on the batteries lifetime in the hybrid system design.

The batteries lifetime is estimated according to previous works [20]. The Rainflow counting method is applied to the battery energy, estimated from simulations or experimental results, to quantify the number of cycles applied to the batteries. The Miner's rule is used at the end to estimate the batteries lifetime.

5. Storage Energy Management

Qualitatively, each storage device has a proper reaction time according to Ragone theory [21]. Thus, in the time horizon of the wind energy, it is possible to assign a storage device suitable for each segment corresponding to its dynamics.

In this approach of storage devices integration in wind-PV-diesel hybrid system, wind power can be divided into three components. The current supplied by the wind generator to the DC-bus is assumed as a sum of low frequency component IBF, middle frequency component IMF and high frequency component IHF. The high frequency components are allocated to UC, and the medium frequency components are mitigated by the batteries. In this case, the DG provides the difference between the load demand and the mean value of wind power. These components are expressed in (9).

$$\begin{cases} I_{wo} = I_{BF} + I_{MF} + I_{HF} \\ I_{bato} = I_{MF} \\ I_{uco} = I_{HF} \\ I_{do} = I_L - I_{BF} \end{cases} \quad (9)$$

Two low-pass filters are used to obtain the three components of the wind power. The filters frequencies are f1 and f2, with f1> f2. The UC and battery reference currents are generated according to Fig.6. The control strategies of the power converters are detailed in previous works [10,11,20].

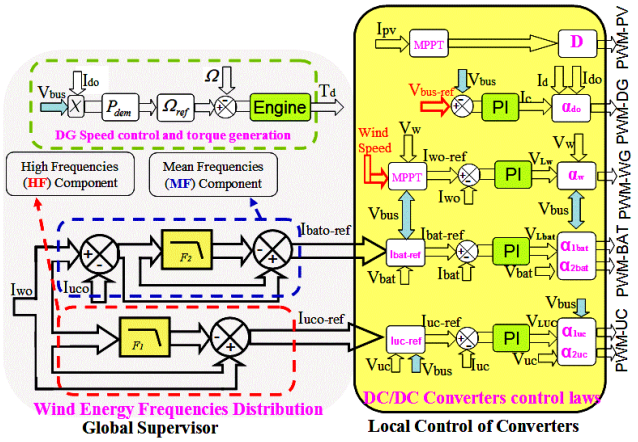

Fig. 6. Control strategies for energy management

6. Simulation Results

The hybridization criteria are applied to the *DG* mission in the no-storage system by using the *WG*, the load and the *PV* powers presented in Fig.7 and Fig.11. The following values are obtained: *PHF=57%* and *EHF=20mHz*. These results show that the *DG* mission is favorable to hybridization by using storage devices.

Simulations are performed to illustrate the efficiency of the proposed strategy of energy management in a wind-PV-DG-UC-batteries system. A fluctuating power is provided by the *WG* as presented in Fig.7. The used wind speed profile for hybrid system simulations is presented in [1]. The *WG* system operates at the maximum power as shown by Fig.8.

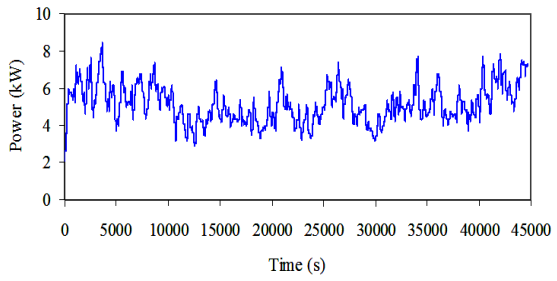

Fig. 7. Power provided by the *WG*.

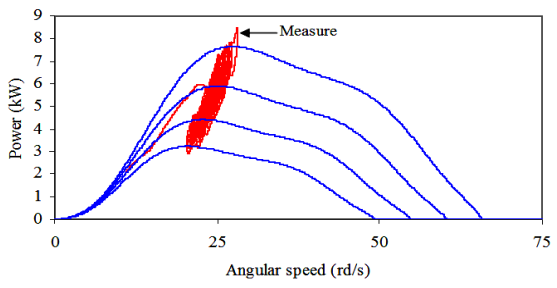

Fig. 8. WG power as function of rotating speed.

In Fig.9, it can be observed that the PV system operates at its maximum power for each value of solar radiation. The disturbances induced by the WG power on the DC-bus are effectively absorbed by the storage units as shown in Fig.10.

It can be observed that the major part of the micro-cycles is smoothed by the UC. Doing this, the batteries cycles are greatly reduced and their lifetime improved.

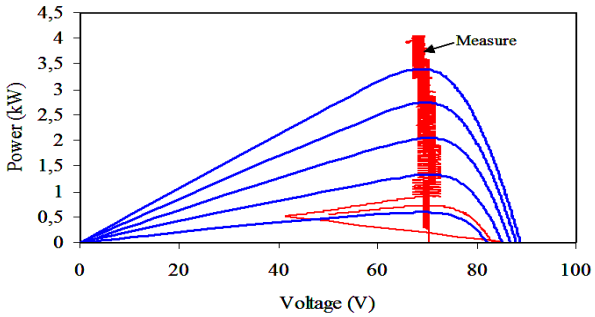

Fig. 9. PV power as function of PV voltage

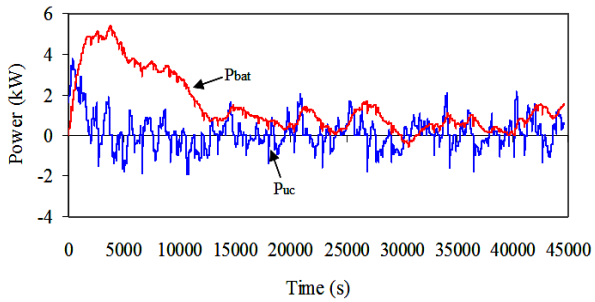

Fig. 10. Stored power by *UC* and batteries.

In Fig.11, it can be observed that the DG power is smoothed and varies according to load (PLoad), PV (PPV), and WG powers variations. Fig.12 presents the DC-bus voltage control result; which is well regulated around 110V from the DG. This confirms the good efficiency of the energy management and of the power converters control method.

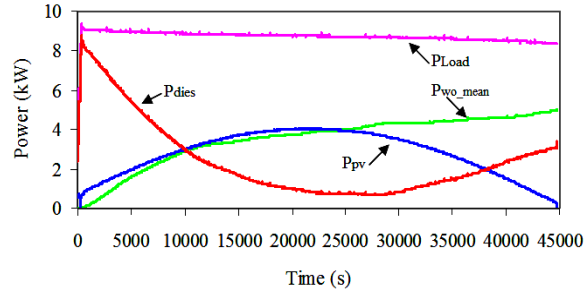

Fig. 11. Load, DG and PV powers.

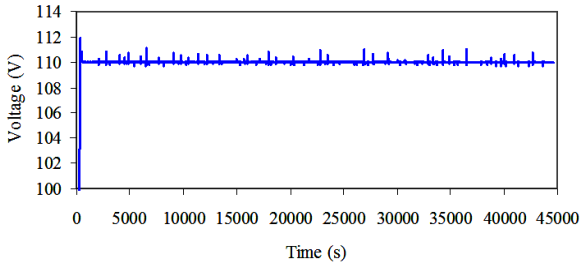

Fig. 12. *DC-bus* voltage regulated around *110V* by the *DG*.

7. Experimental Setup and Results

The designed experimental setup includes a WG emulator, a PV panels, a DG emulator (power source), an UC module, a batteries and an electric load as shown in Fig.13. The control algorithms of the DC/DC converters are implemented in PIC18F4431 microcontroller.

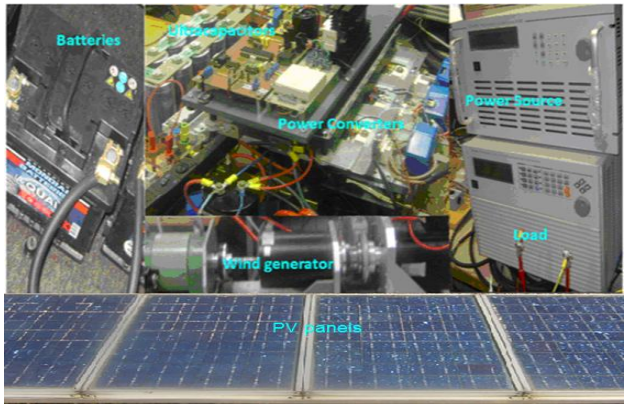

Fig. 13. Hybrid system experimental test bench

The fluctuating current provided by the WG is presented in Fig.14. The major part of the disturbances is absorbed by the UC as shown in Fig.15. The battery's current is less fluctuating than the UC ones as illustrated in Fig.16. The load current and the currents provided to the DC-bus by the DG and by the PV panels are illustrated in Fig.17.

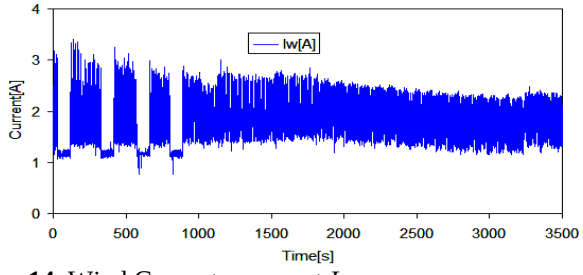

Fig. 14. Wind Generator current I_w

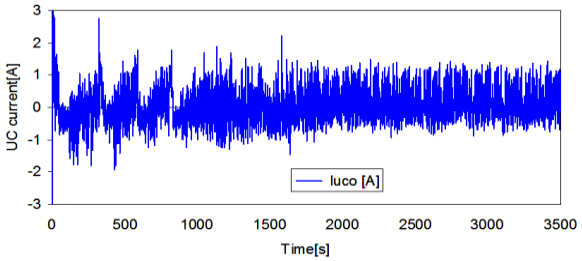

Fig. 15. *UC* current I_{uco}

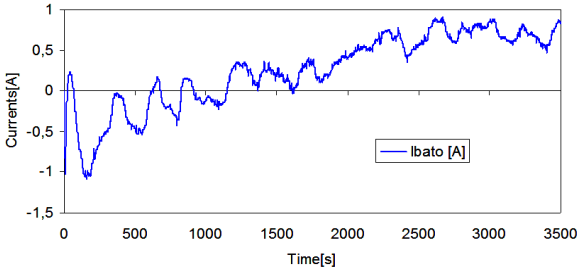

Fig. 16. Battery current Ibato

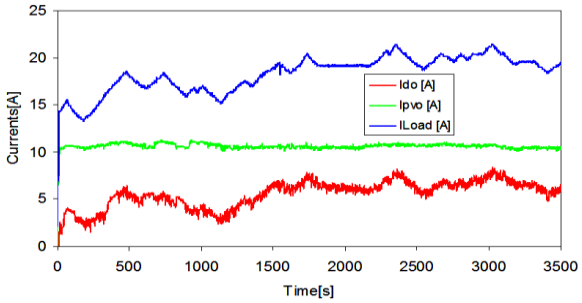

Fig. 17. Electric load, DG and the PV currents

By comparing the currents measured at the common coupling point (Iwo, Iuco, Ibato, Ido, Ipvo, and ILoad), it can be observed that the DG current Ido is smoothed and the WG current fluctuations are absorbed by the UC and batteries. So, as expected, the resulting current from the interaction between the WG and the storage devices has slow variations and corresponds to the mean value of the WG current Iwo. Fig.18 presents the DC-bus and the PV panel voltages. It can be observed that the DC-bus voltage is well regulated around the set-point (48V) by the DG.

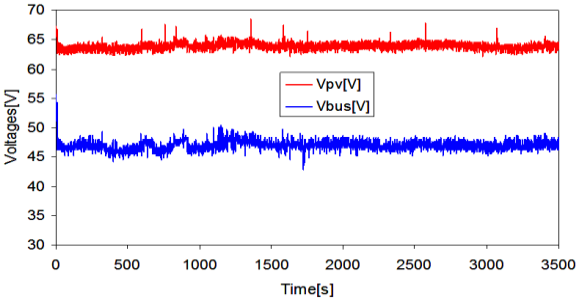

Fig. 18. PV panels and DC-bus voltages

The storage devices (batteries and UC) voltages are plotted in Fig.19. These voltages vary according to the system evolutions.

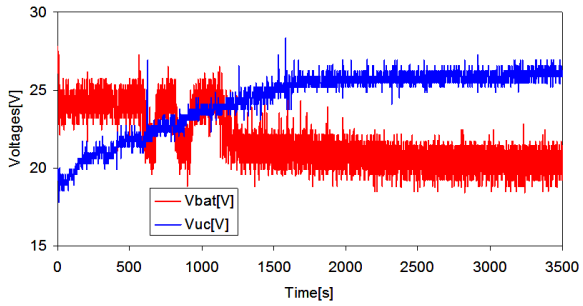

Fig. 19. Battery and UC voltages

8. Conclusion

This paper deals the energy transfer management in a Wind-PV-Diesel hybrid system. The renewable sources (PV and WGE) are operated at their maximum power point. The diesel generator is dedicated to regulate the DC-bus voltage. Interactions between sources are studied and the need of storage units is shown in aims to ensure good performance and stability of the hybrid system. Batteries and Ultracapacitors are used in a complementary mode to mitigate the fluctuating currents induced on the DC-bus. The storage devices sizing strategy, which takes into account the actual conditions of operation, is introduced. Efficiency of the implemented control strategies is shown through some simulation and experimental results analysis.

Acknowledgements

This work was financially supported by "Région Haute Normandie", FRANCE.

APPENDIX EXPERIMENTAL SYSTEM PARAMETERS

Wind generator emulator :

Wind turbine *:R = 1.25 m; ρ= 1.225 kg/m3; λopt = 6*

Wind turbine servo-motor*: Ωmax = 900 rpm; J = 1200 10^{-5} kg m^2; Γn = 31 Nm; In = 7.51 A*

Permanent magnet generator *: Ωn = 420 rpm; In = 2.9 A; P = 6; Γn = 26 Nm; L = 74.475 mH; R = 11.68 Ω*

J = 0.0136 kg m^2;

No load FEM = 21.6 V at 60 rpm.

Buck converter: *L_{in} =100uH, C_w=2200uF; L_{wo}=100uH,* C_{wo}=3.3mF.

PV panels system: 1kWc

Cpv=3.3mF , Lpvo=100uH.

Storage devices :

Ultracapacitors :

Boostcap 2600 MAXWELL ,10 cells of 2.7V; L_{uc}=100uH, C_{uco}=3.3mF

Batteries :

2 modules of 12V in series; L_{bat}=100uH, C_{bato}=3.3mF.

Electric programmable load *: Chroma Programmable AC/DC Electronic Load : model 65804/4.5kW/45A/350V*

Diesel generator emulator :

Chroma Programmable AC/DC Power Source : model 61505/0~300V/ 4KVA

References

[1] C. Nichita, D. Luca, B. Dakyo, and E. Ceanga, "Large band simulation of the wind speed for real time wind turbine simulators", *IEEE Trans. Energy conversion*, vol. 17, n. 4, pp. 523- 529, Dec 2002.

[2] T. Burton, D. Sharpe, and E. Bossanyi, *Wind Energy Handbook*, London: Wiley, 2001.

[3] T. Tanabe, *et al.* "Generation Scheduling for wind power generation by storage battery system and meteorological forecast", *the 21st Century IEEE Power and Energy Society (PES 2008) General Meeting - Conversion and Delivery of Electrical Energy*, pp. 1-7, Jul. 2008.

[4] J. Apt, "The spectrum of power from wind turbines", *Power Sources Journal*, vol. 169, pp. 369-374, 2007.

[5] B. G. Rawn, P. W. Lehn, and M. Maggiore, "Control methodology to mitigate the grid impact of wind turbines", *IEEE Trans. Energy Conversion*, vol 22, n. 2, Jun. 2007.

[6] C. Luo, H. G. Far, H. Banakar, P. Keung, and B. Ooi, "Estimation of wind penetration as limited by frequency deviation", *IEEE Trans. Energy Conversion*, vol. 22, n. 3, pp. 783-791, Sept. 2007.

[7] Z. Chlodnicki, W. Koczara, and N. Al-Khayat, "Hybrid UPS Based on Supercapacitor Energy Storage and Adjustable Speed Generator", *Electrical Power Quality and Utilization Journal*, Vol. XIV, n. 1, 2008

[8] Y. Cheng, J. Van Mierlo, P. Lataire, "Test Platform for Hybrid Electric Vehicle with the Super Capacitor based Energy Storage, *International Review of Electrical Engineering IREE,* vol. 3. n. 3, pp. 466-478, Juin 2008.

[9] J. H. Lee, S. H. Lee, and S. K. Sul, "Variable-speed engine generator with supercapacitor: Isolated power generation system and fuel efficiency", *IEEE Trans. Ind. applications,* vol. 45, n. 6, pp. 2130-2135, Dec. 2009.

[10] A.M. Tankari, M.B. Camara, B. Dakyo, and C. Nichita, "Ultracapacitors and Batteries Integration in Wind Energy Hybrid System - Using the Frequencies distribution Method", *International Review of Electrical Engineering IREE* vol.5, no. *2,* pp. 521-529, March-April 2010.

[11] M. A. Tankari, M.B. Camara, B. Dakyo, and C. Nichita, "Power Fluctuations Attenuation in Wind-PV-Diesel Hybrid System – Ultracapacitors and Batteries", International Review of Electrical Engineering IREE, Vol.5, No. 5, ISSN 1827 - 6679, October 2010.

[12] M. El Mokadem, "Modélisation et simulation d'un système hybride pour un site isolé. Problématique liée aux fluctuations et variations d'énergie au point de couplage," *PhD dissertation, GREAH laboratory, Université du Havre, France*, 2006.

[13] M. A. Tankari, "Système Multi-sources de Production d'Énergie Électrique Méthode de Dimensionnement d'un Système Hybride et Mise en œuvre Expérimentale de l'Optimisation de la Gestion d'Énergie," *Ph.D. dissertation, GREAH laboratory, University of Lehavre*, 2010.

[14] C. R. Akli, "Conception systémique d'une locomotive hybride autonome. Application à la locomotive hybride de démonstration et d'investigations en énergétique LHyDIE développée par la SNCF," *PhD thesis, INPT, University of Toulouse*, 2008.

[15] MAXWELL Technologies, "Product guide-maxwell technologies boostcap ultracapacitors," available : http://www.maxwell.com/pdf/1014627BOOSTCAPProductGuide.pdf, Doc. No. 1014627.1, 2009.

[16] Hammar, A. Venet, P. Lallemand, R. Coquery, G. and Rojat, G., "Study of Accelerated Aging of Supercapacitors for Transport Applications," *IEEE Trans. Ind. Electronics,* vol. 57, no.12, pp. 3972 – 3979, Dec. 2010.

[17] A. Jossen, "Fundamentals of battery dynamics", *Power Sources J., vol. 154,* pp. 530–538, 2006.

[18] H. Wenzl, et al., "Life prediction of batteries for selecting the technically most suitable and cost effective battery", *Power Sources J., vol. 144*, pp.373–384, 2005.

[19] Bindner H., T. Cronin, P. Lundsager, J. F. Manwell, U. Abdulwahid, and I. Baring-Gould, "Benchmarking - lifetime modelling," enk6-ct-2001-80576. Riso National Laboratory, Denmark, 2005.

[20] M. A. Tankari, M.B.Camara, B. Dakyo, C. Nichita, "Wind Power Integration in Hybrid Power System with Active Energy Management," *Int. Journal for Computation and Mathematics in Electrical and Electronic Engineering (COMPEL),* Vol. 30, No. 1, pp. 245-263, 2011.

[21] T. Christen and Martin W. Carlen, "Theory of ragone plots," *Int. Journal on Power Sources* , vol. 91, no. 2, pages 210_216, Dec. 2000.

Nomenclature

PMSM	Permanent Magnet Synchronous Machine
DG	Diesel Generator Emulator
WG	Wind Generator Emulator
UC	Ultracapacitors
W_s	Wind speed
MPPT	Maximum power point tracking
λ_{opt}	Optimum value of the tip speed ratio
Φ_{max}	Generator maximum flux
ρ	Air density
p	Number of pole pairs per phase
R	Turbine radius
C_Γ	Torque coefficient
I_{wo}	WG current provided to the DC-bus
I_L	Load current
I_{do}	DG current provided to the DC-bus
V_w	WG rectified voltage
I_w	WG rectified current
I_{woF1},I_{woF2}	Filter F1 and F2 output current, respectively
f_i	Filter cut-off frequency, fi=1/(2.π.τi), i={1;2}
ρ_p	Power density of the considered source
ρ_e	Energy density of the considered source
τ_i	Time constant of the filter
V_{bus}	DC-bus voltage
P_{pv}	Photovoltaic (PV) panel power
I_{pv}	PV panel current
V_{pv}	PV panel voltage
V_t	Thermal potential
A	Ideal constant of the diode
R_s	Equivalent series resistance
R_{sh}	Equivalent shunt resistance
I_{sat}	Saturation current
I_{ph}	Photocurrent
D	PV converter duty cycle
Δd	Step variation of duty cycle D
P^*	PV panel reduced power ($P_{pv}=V_{bus}*I_{pv}/D$)